Proceedings of the 14th International Heat Transfer Conference
IHTC14
August 8-13, 2010, Washington, DC, USA

IHTC14-23079

TRANSPORT PROCESS STUDY IN SODIUM ALANATE HYDROGEN STORAGE SYSTEM DURING DESORPTION

Maha Bhouri, Jacques Goyette
Institut de Recherche sur l'Hydrogène, UQTR
Trois-Rivièrs, Québec, Canada

Bruce J. Hardy, Donald L. Anton
Savannah River National Laboratory
South Carolina, United States

ABSTRACT

Transport processes in a sodium alanate hydrogen storage system during desorption are presented. The mathematical model, which considers heat conduction and convection, hydrogen flow governed by Blake-Kozeny law and the chemical kinetics, is solved using the COMSOL Multiphysics® finite element software. The numerical simulation is used to present the time-space evolutions of the temperature, pressure and hydride concentration. The results are discussed for two cases: a finned storage system and a finless one. It is shown that the whole process occurring in the bed is governed and controlled by heat transfer from the heating fluid to the storage media and strengthened by axial heat transfer through the fins. The importance of the hydride bed thermal conductivity has also been evaluated. It was observed that the hydrogen discharge rate in a finless system can be improved if we find ways of increasing the thermal conductivity of the storage media. On the other hand, for a reservoir with fins, heat transfer is good enough that the discharge rate is limited by the kinetics.

INTRODUCTION

A metal hydride reaction is a reversible process where hydrogen can be charged or discharged at moderate temperatures and pressures with a substantial enthalpy change. During charging, heat of reaction has to be removed, while for the discharge of hydrogen, heat has to be added. The rates at which these reactions proceed depend on the transport of heat and are generally limited by the poor thermal conductivity of the hydride bed. Hence, the subject of heat transfer enhancement is of crucial interest in designing hydrogen storage systems to meet the DOE performance targets in terms of charging/discharging time, gravimetric and volumetric capacities allowing the extension of metal-hydrogen systems from laboratory to industry [1]. While experimental design of metal hydride reactors has been the subject of several research projects, this approach remains expensive and is limited to a narrow range of configurations and storage media. In addition, measurements obtained from experimental studies do not give a complete picture of the coupled physical phenomena occurring in the storage system. Numerical investigations, however, are considerably more flexible taking into account the interactions between heat and mass transfer along with accompanying reaction kinetics. Further, numerical models can be readily modified for application to various types of hydrides and storage vessel configurations. Numerical models can also be used to perform sensitivity analysis to identify physical and geometrical parameters of the media and vessel that optimize the performance of the reservoir.

BACKGROUND

A number of numerical models have previously been developed for metal hydride based hydrogen storage.

Demircan et al [2], Ataer et al [3] investigated various bed geometries for the hydriding process with the goal of reducing the charging time. Dogan et al. [4] presented a mathematical model describing the absorption of hydrogen in a metal hydride bed sandwiched between two cooling regions and studied the effect of two feed systems on filling time. They found that hydrogen supplied radially from both sides of the bed resulted in a high charging rate.

Kikkinides et al. [5, 6] attempted to improve the design and the control of metal hydride beds by integrating a cooling medium model and introducing additional heat exchangers at a concentric inner tube and annular ring inside the tank.

Heat and mass transfer in a metal hydride storage system equipped with a single concentric cooling tube and fins has been investigated by a number of research groups [7-10]. MacDonald et al [7] investigated the desorption process for

three reservoir configurations intended to feed a fuel cell with hydrogen: without heat enhancement, with radial external fins and an annular reservoir. The annular tank, in addition of offering the most compact system, met the requirements of feeding a fuel cell at an acceptable pressure. The effect of introducing external and internal fins was studied by Askri et al [8] and results showed that by combining a concentric heat exchanger and internal radial fins an 80% improvement in the storage time could be achieved. Mellouli et al [9] studied a configuration similar to that of Askri, but instead of utilizing the fins, the tank was equipped with metal foam and exchanged heat with its surroundings. Their results showed that metal foam significantly increased the effective thermal conductivity of the bed and, thus, the rate of heat transfer. In other studies [11, 12], the same authors conducted experimental and numerical investigations of a metal hydride storage system equipped with a spiral heat exchanger. Different designs were compared by taking into account the heat exchange of the system with cooling fluid through its lateral area and with the ambient environment at its base. In order to improve the thermal conductivity of the magnesium hydride, Chaise et al [10] used porous metal hydride compact technology in which a compacted disk of magnesium hydride was combined with expanded natural graphite (ENG). A comparison between two reservoirs filled with compacted disks containing respectively 5wt% of ENG layered between copper fins and 20wt% of ENG without fins, showed similar performance in terms of loading time. This result was promising since the weight capacity of the storage system is markedly improved with the omission of fins.

The shell and tube configuration for a hydrogen storage system consists of multiple heat exchanger tubes embedded in a cylindrical metal hydride tank. The absorption process in this configuration was studied by Mohan et al [13]. Their results showed that the bed thickness is the dominating geometric parameter governing the performance of the hydrogen storage device.

Krokos et al [14] developed a 3-dimensional Cartesian mathematical model to describe hydrogen storage in a metal hydride reactor for which the hydride was contained in multiple tubes. The metal hydride bearing tubes were embedded in a cylindrical tank and heat transfer fluid was allowed to flow externally to the tubes. An optimization study showed that 9 hydride tubes distributed uniformly in the heat transfer fluid having a velocity of 1m/s, yielded the optimal charging rate.

Hardy et al [15] developed a general model to describe heat and mass transfer in a finned shell and tube hydrogen storage vessel. Heat removal from the hydride bed was effected by 9 tubes containing heat transfer fluid. In the 3-dimensional form of the model thin transverse fins were used to enhance bed heat transfer; fins were not present in the 2-dimensional form. Hydrogen was introduced to the bed via 8 porous walled recovery tubes. The hydride powder occupied the space between the tubes and the wall of the cylindrical storage vessel. The storage media considered in the model was $TiCl_3$ catalyzed $NaAlH_4$. The difference in the rate of hydrogen uptake between the 2-dimensional (no fins) and 3-dimensional (with fins) models highlights the importance of heat transfer to the charging process [16].

Most of the work summarized in this literature review focused on the uptake of hydrogen during charging of the storage vessel. However, because the storage tank must also discharge hydrogen to power a fuel cell, it is important to evaluate system performance during the liberation of hydrogen from the hydride. Further, the densification of the hydride powder is essential if one wishes to achieve packing densities consistent with gravimetric and volumetric requirements. However, radial fins, which enhance heat transfer, can become distorted during the densification process. For this reason, we investigate whether increasing the hydride thermal conductivity in a vessel without fins can reproduce the performance of a finned system during the discharge process.

MATHEMATICAL MODEL

The model developed by Hardy et al [15, 16] is considered here to investigate numerically the two and three-dimensional transient heat and mass transfer during the desorption process within the sodium alanate hydride bed. In the first part of the paper, a mathematical model describing coupled heat and mass transfer in the bed is presented. In the second part, we show the results of simulation including the time-space evolutions of the temperature and hydride concentrations where the storage media is equipped with fins or not. In both cases, we study also how the thermal conductivity affects the heat and mass transfer processes.

The geometric configuration of the hydride bed is similar to the storage system developed and tested by the United Technologies Research Center™ (UTRC™) [17]. As mentioned above, the hydride bed consists of sodium alanate hydride layered between fins that are press-fit to the heat exchange tubes. Since the desorption of hydrogen is endothermic, the heat supply is ensured by a heating fluid flowing through the heat exchange tubes and the released hydrogen will flow in porous filters as is illustrated in Fig.1.

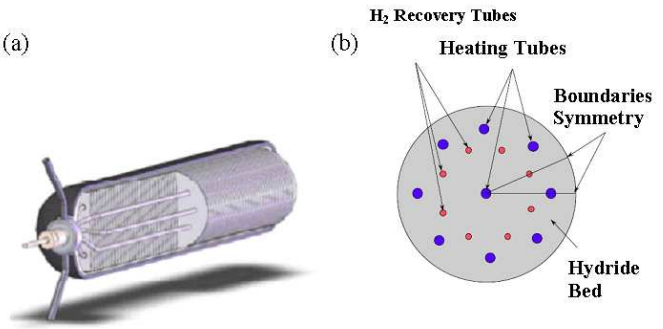

FIGURE 1. (a) SHELL, TUBE AND FIN HYDRIDE BED CONFIGURATION, MOSHER ET AL.[16], (b) CROSS-SECTION OF THE HYDRIDE BED USED IN THIS STUDY

For a hydride layer placed at a sufficient distance from the hemispherical end caps of the vessel, axial and azimuthal

symmetry conditions can be applied and the modeled geometry is reduced to the portion of reservoir showed in Fig.2. The geometric properties of the hydride bed are listed in Tab.1.

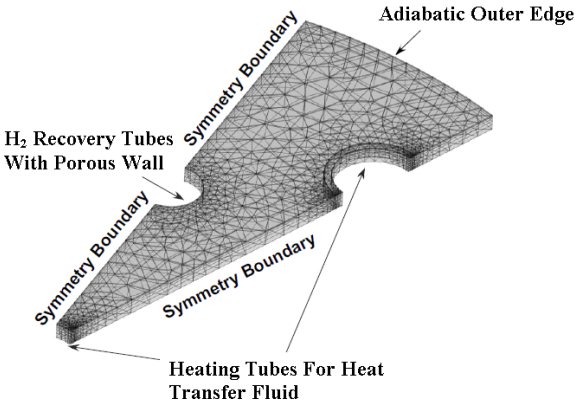

FIGURE 2. GEOMETRY USED FOR COMPUTATIONS IN THE 3-DIMENSIONAL MODEL

The desorption of hydride occurs according to these two steps

$$\underbrace{NaAlH_4}_{Species1} \underbrace{\leftrightarrow}_{Reaction1} \underbrace{\frac{1}{3}Na_3AlH_6}_{Species2} + \frac{2}{3}Al + H_2 \underbrace{\leftrightarrow}_{Reaction2} \underbrace{NaH}_{Species3} + Al + \frac{3}{2}H_2 \quad (1)$$

In the following, C_1, C_2 and C_3 are respectively the concentrations of species $NaAlH_4$, Na_3AlH_6 and NaH. The forward and backward reaction rates r_{1F}, r_{1B}, r_{2F} and r_{2B} are respectively

$$r_{1F} = C_{eqv} A_{1F} \exp\left[-\frac{E_{1F}}{RT}\right]\left[\frac{P(C,T) - P_{eq1}(T)}{P_{eq1}(T)}\right] \quad (2)$$

$$r_{1B} = -C_{eqv} A_{1B} \exp\left[-\frac{E_{1B}}{RT}\right]\left[\frac{P_{eq1}(T) - P(C,T)}{P_{eq1}(T)}\right] \quad (3)$$

$$r_{2F} = -C_{eqv} A_{2F} \exp\left[-\frac{E_{2F}}{RT}\right]\left[\frac{P(C,T) - P_{eq2}(T)}{P_{eq2}(T)}\right] \quad (4)$$

$$r_{2B} = C_{eqv} A_{2B} \exp\left[-\frac{E_{2B}}{RT}\right]\left[\frac{P_{eq2}(T) - P(C,T)}{P_{eq2}(T)}\right] \quad (5)$$

$P_{eq1}(T)$ and $P_{eq2}(T)$ are the equilibrium H_2 pressures based on the van't Hoff equation

$$P_{eq1}(T) = 10^5 \exp\left[\frac{\Delta H_1}{RT} - \frac{\Delta S_1}{R}\right]$$
$$P_{eq2}(T) = 10^5 \exp\left[\frac{\Delta H_2}{RT} - \frac{\Delta S_2}{R}\right] \quad (6)$$

The kinetics model of the sodium alanate hydride was developed by the United Technologies Research Center ™ (UTRC™). It is expressed in terms of partial differential equations that depend on the reaction rates of formation and dissociation of each species.

$$\frac{dC_1}{dt} = \begin{cases} r_{1F}\left[\frac{3C_2(t)}{C_{eqv}} - C_{2sat}(T)\right]^{\chi_{1F}} & if\ P \geq P_{eq1}(T) \\ r_{1B}\left[\frac{3C_1(t)}{C_{eqv}}\right]^{\chi_{1B}} & if\ P < P_{eq1}(T)\ and\ C_1(t) \geq 0 \end{cases} \quad (7)$$

$$\frac{dC_3}{dt} = \begin{cases} r_{2F}\left[\frac{3C_3(t)}{C_{eqv}} - C_{3sat}(T)\right]^{\chi_{2F}} & if\ P \geq P_{eq2}(T) \\ r_{2B}\left[\frac{3C_2(t)}{C_{eqv}}\right]^{\chi_{2B}} & if\ P < P_{eq2}(T)\ and\ C_2(t) \geq 0 \end{cases} \quad (8)$$

In the UTRC™ study, hydrogen charging curves for pure NaH were generated for different values of temperatures and pressure and compared to data given by UTRC™ and good agreement was obtained. For the sake of brevity, the reader is referred to the evaluation of the kinetics model in Hardy, et al [15, 16].

Parameter	Value
Hydride bed diameter	23.00cm
Diameter of heating tubes	1.91cm
Diameter of H_2 recovery tubes	1.27cm
Number of heating tubes	9
Number of H_2 recovery tubes	8
Thickness of fin plates	0.0313cm
Spacing between fin plates	0.63cm
Tube wall thickness	0.12cm
Density of tube and fin material	2.7g/cm^3

TABLE 1. GEOMETRIC PROPERTIES OF THE STORAGE SYSTEM

The mathematical model for the storage reservoir is based on the following assumptions:

1. Only hydrogen is allowed to flow in the system.
2. The media bed does not expand or contract. This assumption is especially significant as media proposed for hydrogen storage experiences contraction during hydrogen discharge.
3. The thermal properties of the bed do not change with the amount of hydrogen release.
4. The thermo-physical proprieties are independent of bed temperature and concentration.
5. The characteristics of the bed are unaffected by the number of loading–unloading cycles. That is, aging/cycling of the media is neglected.

6. Heat transfer from the bed occurs via the heat transfer fluid, by convection to the hydrogen in the recovery tubes, and by homogeneous heat exchange with hydrogen flowing through the bed.
7. There is local thermal equilibrium between the hydride and hydrogen gas.
8. The thermal conductivity, specific heat and viscosity of hydrogen do not vary with pressure over the operational regime of the storage system.
9. The tubes and fins are composed of 6063 T83 aluminium.
10. Thermal contact between the bed and the cooling tubes, the bed and the fin, and the fin and the cooling tubes is good, i.e. thermal contact resistance is neglected.
11. The bed void fraction remains constant and uniform throughout.
12. The bed fills the entire volume of the space between the fins and tubes.
13. The bulk temperature of the heat exchange fluid and the hydrogen recovered from the bed is constant and uniform.
14. The hydrogen flows through the recovery tubes.
15. Hydrogen is assumed as in ideal gas as the pressure within the bed is moderate.
16. Axial end effects have negligible impact on the performance of the storage system.

Equations describing heat and mass transfer in the hydride bed can be expressed in the general form

$$\frac{\partial}{\partial t}(a_1\phi)+\nabla.\left(a_2\vec{V}\phi\right)=\nabla\left(\Gamma_\phi\nabla\phi\right)+S_\phi \tag{9}$$

The meaning of the terms in Eq.(7) are given for the hydride bed, tubes and fins in Tab.2.

Equations	ϕ	a_1	a_2	Γ_ϕ	S_ϕ
Hydrogen mass balance	C_{nd}	1	1	0	$\frac{1}{\varepsilon C_{ref}}\left(\frac{1}{2}\frac{dC_3}{dt}-\frac{dC_1}{dt}\right)$
Bed energy balance	T_{nd}	$\rho_{bed}C_{p\,bed}+\varepsilon\rho_{H_2}C_{p\,H_2}$	$\varepsilon\rho_{H_2}C_{p\,H_2}$	k_{bed}	$\frac{1}{T_{ref}}\left(\frac{\partial P}{\partial t}+\varepsilon\vec{V}.\nabla P\right)+\frac{1}{T_{ref}}S_{T_{nd}}$ $S_{T_{nd}}=\frac{dC_1}{dt}\Delta H_{Rxn1}-0.5\frac{dC_3}{dt}\Delta H_{Rxn2}$
Energy balance for tubes and fins	T_{metal}	$\rho_{metal}C_{p\,metal}$	*0*	k_{metal}	*0*

TABLE 2. SPECIFIC FORMS OF THE GENERAL CONSERVATION EQUATION

The hydrogen is considered as an ideal gas and the equation of state for the gas phase is expressed by the ideal gas law

$$P=CRT \tag{10}$$

To describe the hydrogen flow within the metal hydride bed, the Blake-Kozeny equation is modified to obtain the mean interstitial velocity, rather than the superficial velocity

$$\vec{V}=\frac{D_p^2}{150\mu}\left(\frac{\varepsilon}{1-\varepsilon}\right)^2\nabla P \tag{11}$$

Initial and Boundary Conditions

Initially, metal hydride, fins and tubes are at a uniform temperature of 120°C. The hydride bed, initially at a pressure of 50 bar, is composed of three species $NaAlH_4$, Na_3AlH_6 and NaH having respectively initial concentrations of 6650 mol/m^3, 90 mol/m^3 and 6427.15 mol/m^3. These values are obtained from the 0-kinetics model for a fully loaded reservoir, see Hardy et al [15]. During the desorption process, the extraction of hydrogen from the hydride bed is driven by the decrease in gas pressure in the hydrogen recovery tubes which will go from 50 to 1 bar.

On the walls and surfaces of symmetry, the Neumann boundary condition is applied

$$\left(C_{nd}\vec{V}\right).\vec{n}=0 \tag{12}$$

On the hydrogen recovery tube wall joining the bed, we have

$$C_{nd}=\frac{P_{rec}T_{ref}}{P_{ref}\,T_{wall}} \tag{13}$$

All exterior boundaries and surfaces of symmetry are thermally insulated

$$\vec{n}.\nabla.\left(k_{bed}\nabla T_{nd}\right)=0 \tag{14}$$

There is convective heat transfer through the lateral area of the heat exchange tubes and the hydrogen recovery tubes in contact with the hydride bed

$$\vec{n}.\left(k_{metal}\nabla T_{metal}\right)=-h_{conv\ heat}\left(T_{Wall}-T_{heat\ bulk}\right) \tag{15}$$

$$\vec{n}.\left(k_{bed}\nabla T_{nd}\right)=-h_{H_2}\left(\frac{T_{wall}-T_{H_2\ bulk}}{T_{ref}}\right) \tag{16}$$

The convective heat transfer coefficients are calculated with the Dittus-Boelter correlation

$$h = \frac{Nu_D k}{D},\ Nu_D = 0.023 \mathrm{Re}_D^{\ 0.8}\ \mathrm{Pr}^{0.4},\ \mathrm{Re}_D = \frac{\rho V D}{\mu} \qquad (17)$$

The continuity condition is applied at the interfaces between fins/tubes and tubes/hydride bed

$$\nabla.\left(k_{metal1} \nabla T_{metal1}\right) = \nabla.\left(k_{metal2} \nabla T_{metal2}\right) \qquad (18)$$

$$\nabla.\left(k_{metal} \nabla T_{metal}\right) = \nabla.\left(k_{bed} \nabla T_{bed}\right) \qquad (19)$$

This set of equations, with their relative initial and boundary conditions, are solved using COMSOL Multiphysics®, version 3.5a [18], a commercial software based on the Finite Element Method(FEM).

RESULTS

Fig.3 shows plan and isometric views of the temperature profile in the 3-dimensionnal model after 720 s. The left image shows the temperature evolution from the midplane of the hydride layer to the midplane of the fin. The plan view, on the right, is the temperature distribution over the midplane of the hydride layer. It is clear that the hydride bed is cooled due to the endothermic process of hydrogen desorption. Moreover, the bed area around the heating tubes have a higher temperature than the others regions. Throughout the transient, the temperature of the heat transfer fluid is maintained at 120°C which promotes higher rate of hydrogen discharge in this area.

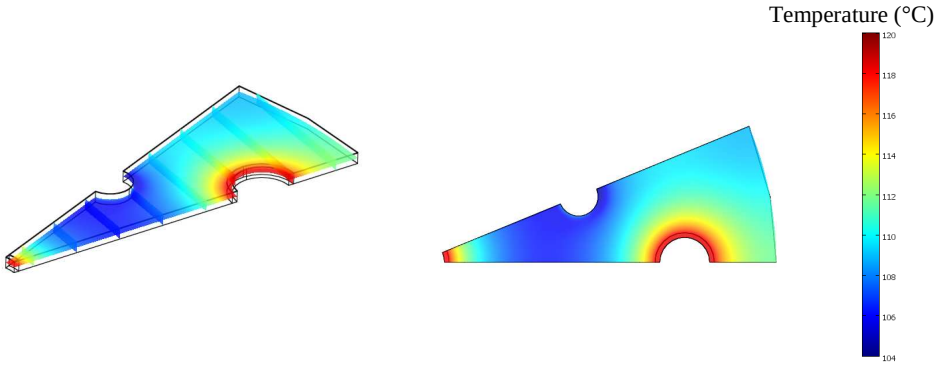

FIGURE 3. ISOMETRIC AND PLAN VIEWS OF TEMPERATURE PROFILE FOR 3-DIMENSIONAL MODEL AT 720 s. BASE OF ISOMETRIC FIGURE IS AT BED MIDPLANE (CENTER OF THE HYDRIDE BED LAYER BETWEEN FINS)

Figs.4 (a,b) compare the distribution of the hydride bed temperature between the 2-dimensional model (without fins) and the bed midplane of the 3-dimensional model (with fins) at 720 s. Figures 5.(a,b) and (c,d) compare the concentration of $NaAlH_4$ and Na_3AlH_6 for the 2-dimensional model (without fins) and the bed midplane of the 3-dimensional model (with fins) at 720 s.

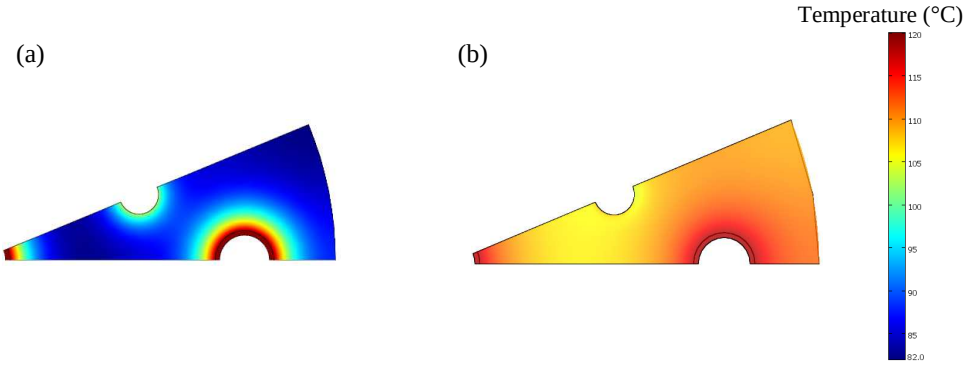

FIGURE 4. COMPARISON BETWEEN 2-DIMENSIONAL (WITHOUT FINS) AND 3-DIMENSIONAL (WITH FINS) BED MIDPLANETEMPERATURE AT 720 s. FIGURE 4a REPRESENTS THE 2-D MODEL AND FIGURE 4b REPRESENTS THE 3-D MODEL.

Fig.4a shows that after 720 s, except the areas very close to the heating tubes, the rest of the hydride bed is at a temperature around 90°C. This indicates that transport of heat from the heating fluid to the rest of the hydride bed is limited by the poor

thermal characteristics of the latter. This is reflected on the formation/decomposition of the products/reactants. As seen from Eq.1, the discharge of hydrogen takes place in two successive decomposition reactions for $NaAlH_4$ and Na_3AlH_6. The hexahydride acts as a reactant and a product simultaneously. Initially, concentrations of $NaAlH_4$ and Na_3AlH_6 are respectively 6650 and 90 mole/m^3. After 720 s, they are respectively around 6000 and 300 mole/m^3 (see Fig.5.a and c); this is due to the slow reactions caused by ineffective heat transfer. As seen from Fig.4b, for the finned system, the temperature at the midplane of the hydride layer has a homogeneous distribution and is above 105°C which is favorable for the desorption process. Indeed, the concentration distribution for tetra and hexa-hydrides reach values around 3500 and 900 mole/m^3 (see Fig.5.b and d); which shows that the introduction of fins allows much higher heat transfer and will result in better use of the hydride bed. The Na_3AlH_6 is supposed to be decomposed into NaH. However, as we explain later, the rate of this reaction is very slow so that the production of this species is not as significant and thereafter it is not shown.

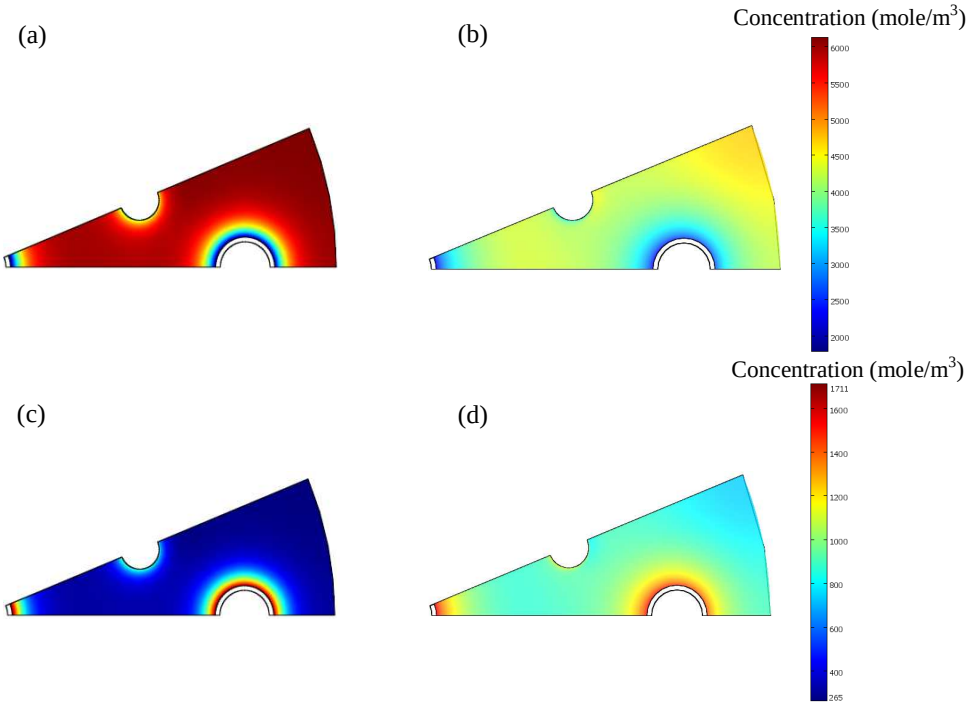

FIGURE 5. COMPARISON BETWEEN 2-DIMENSIONAL (WITHOUT FINS) AND 3-DIMENSIONAL (WITH FINS) $NaAlH_4$ CONCENTRATION (a,b) AND Na_3AlH_6 CONCENTRATION (c,d) AT 720 s. FIGURES5a AND 5d REPRESENT THE 2-D MODEL AND FIGURE 5b AND 5d REPRESENT THE 3-D MODEL.

To better understand the impact of the integration of fins into the hydride bed, the time evolution of the average bed temperatures, equilibrium pressures and hydride pressures are plotted in Figs.6-8 for the two cases, finned and finless systems.

As seen in Fig.6, the average bed temperature profile can be divided into two stages. For the initial stage, the desorption process is characterized by a gradual decrease in the average bed temperature to reach its minimum of 107.17°C after 120 s for the case with fins and 89.94°C after 680 s for the case without fins. After reaching this minimum, the temperature will tend to increase to the temperature of the heating fluid. This behavior is due to the endothermic character of the desorption process: heat must be provided so that the release of hydrogen can still take place.

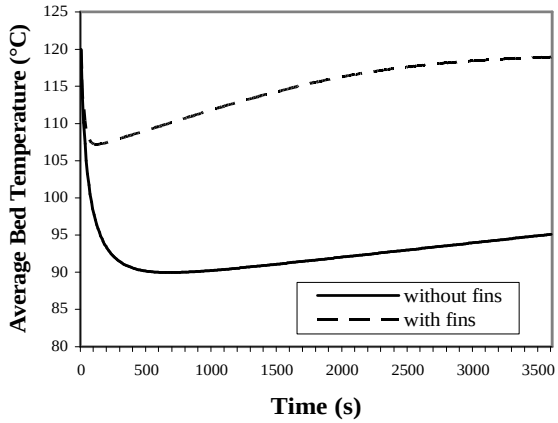

FIGURE 6. COMPARISON OF 2-DIMENSIONAL (WITHOUT FINS) AND 3-DIMENSIONAL (WITH FINS) TRANSIENT AVERAGE TEMPERATURES OF THE HYDRIDE BED

The average equilibrium pressures for reactions 1 and 2 (see Eqs.1 and 6) and the hydride bed pressures for the two cases are presented in Fig.7. As shown, the finned case reaches a higher pressure than the case without fins. On the other hand, the desorption reaction will only proceed if the gas pressure is below the equilibrium pressure of the reactions 1 and 2. This is not the case for the decomposition of Na_3Al_6 to NaH: throughout the desorption, the average equilibrium pressure is below the gas pressure, which means that the dissociation of the hexa hydride makes little contribution to the release of hydrogen. On the other hand, the difference between P and Peq_1 is particularly important for the finned case, resulting in a higher driving force ($1-P/Peq_1$) (see Eq.2) which promotes the dissociation of the tetra-hydride as seen in Fig.5.(a,b)-(c,d). Indeed, from Fig.8, it is clear that the discharge time and the amount of released hydrogen are significantly improved for the finned system.

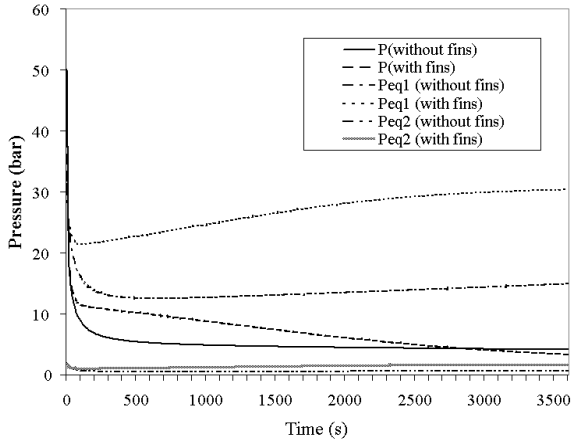

FIGURE 7. COMPARISON OF 2-DIMENSIONAL (WITHOUT FINS) AND 3-DIMENSIONAL (WITH FINS) TRANSIENT AVERAGE EQUILIBRIUM PRESSURES AND GAS PRESSURES

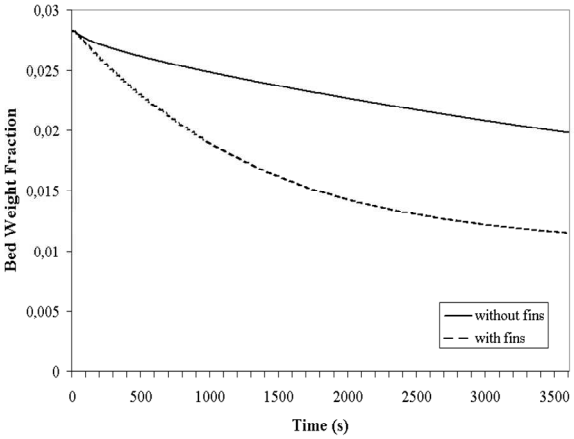

FIGURE 8. COMPARISON OF 2-DIMENSIONAL (WITHOUT FINS) AND 3-DIMENSIONAL (WITH FINS) TRANSIENT AVERAGE WEIGHT FRACTION OF DISCHARGED HYDROGEN

For the system without fins, the discharge of hydrogen is limited by the poor heat transfer characteristics of the hydride bed. Therefore, the enhancement of heat transfer by increasing the bed thermal conductivity from 0.325 W/(m.K) to 5.2 W/(m.K) is examined as shown in Fig.9.

It is clear that for a finned system, an increase in thermal conductivity from 0.325 to 2.6 W/(m.K) has no effect on heat transfer within the hydride bed. For the finless system, increasing the thermal conductivity by a factor of 8 significantly improves the transient evolution of the average temperature of the bed. However, the performance provided by the finned system is not reached.

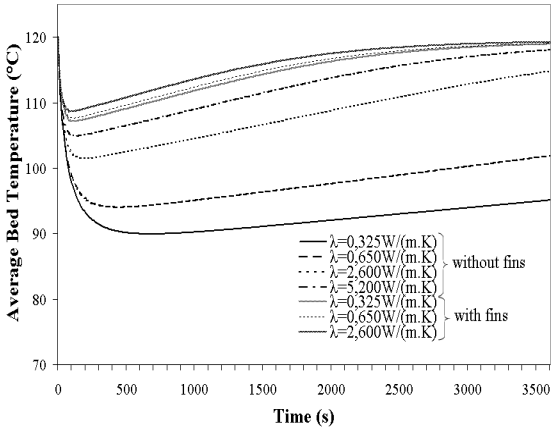

FIGURE 9. EFFECT OF HYDRIDE THERMAL CONDUCTIVITY ON TRANSIENT AVERAGE TEMPERATURES OF THE HYDRIDE BED FOR FINNED AND NO FINNED CASES

.

CONCLUSIONS

A general model describing the heat and mass transfer within a storage system filled with $NaAlH_4$ enabled us to predict the temporal evolution of temperature and concentrations of the various species present in the hydride bed. In spite of the low thermal conductivity of this hydride, the presence of fins permits sufficient transfer to the bed that the limiting factor for hydrogen discharge is the kinetics of hexa-hydride dissociation. In the absence of fins, the heat transfer effected by tubes alone does not support hydrogen discharge rates that match those of the finned system even if, in this last case the thermal conductivity of the bed is increased by a factor of 8. For this reason, it will be interesting to identify other heat exchange systems to achieve optimal rates of hydrogen release and evaluate the best operating conditions such as heating fluid temperature and discharge pressure. This will be the goal of our future work.

ACKNOWLEDGEMENT

M.B. would like to thank the Canadian International Development Agency for a graduate student fellowship. This work was funded in part by the NSERC Hydrogen Canada (H_2CAN) Strategic Research Network and by Natural Resources Canada.

B.J.H. and D.L.A. wish to acknowledge the support and funding of the United States Department of Energy through the Hydrogen Storage Engineering Center of Excellence.

NOMENCLATURE

C	concentration of H_2 in the bed void space, mol H_2/m^3
C_{eqv}	equivalent concentration of $NaAlH_4$ [mol/m^3] based on the initial concentrations of all metal species
C_{nd}	the non-dimensionalized concentration of H_2 = C / C_{ref}
$C_{p\,H_2}$	specific heat of H_2, J/(kg K)
$C_{p\,metal}$	specific heat of the metal, J/(kg K)
C_1	bulk concentration of $NaAlH_4$, mol/m^3
C_2	bulk concentration of Na_3AlH_6, mol/m^3
C_3	bulk concentration of NaH, mol/m^3
D	inner diameter of tube, m
D_p	mean diameter of particles in bed, m
$h_{conv\ heat}$	convection heat transfer coefficient for heat transfer fluid, W/m^2°C
h_{H_2}	convection heat transfer coefficient for H_2 in the feed tube, W/m^2°C
k_{bed}	bed thermal conductivity, W/(m K)
k_{metal}	thermal conductivity of the metal, W/(m K)
$\vec{n}$	outward normal to surface
$Nu_D = \frac{hD}{k}$	Nusselt number based on diameter D
P	pressure, Pa
P_{rec}	H_2 pressure in the recovery tube, Pa
P_{nd}	P / P_{ref} =non-dimensional pressure
$P_{eq1}(T)$	H_2 pressures in equilibrium at temperature, T, with the $NaAlH_4$, Pa
$P_{eq2}(T)$	H_2 pressures in equilibrium at temperature, T, with the Na_3AlH_6, Pa
Pr	Prandtl number
P_{ref}	reference pressure, Pa
R	gas constant =8.314 J/(mol K)
r_{1F}	hydriding (forward) reaction rate coefficient for reaction 1 [mole/(m^3 s)]
r_{1B}	dehydriding (backward) reaction rate coefficient for reaction 1 [mole/(m^3s)]
r_{2F}	hydriding (forward) reaction rate coefficient for reaction 2 [mole/(m^3s)]
r_{2B}	dehydriding (backward) reaction rate coefficient for reaction 2 [mole/(m^3s)]
$\mathrm{Re}_D = \frac{\rho V D}{\mu}$	Reynolds number based on diameter D
$S_{T_{nd}}$	Enthalpy change due to chemical reactions, W/m^3
t	time, s
T	temperature, K
T_h, $T_{heat\ bulk}$	bulk temperature of the heat transfer fluid, K
T_{nd}	T / T_{ref} =non-dimensional temperature
$T_{H_2\ bulk}$	bulk temperature of the H_2 in the recovery tube, K
T_{ref}	reference temperature, K
T_{wall}	tube wall temperature, K
$\vec{V}$	mean interstitial H_2 velocity, m/s

Greek

ΔH_i	enthalpy of reaction on a molar basis of species i, J/(mol of i)
ΔH_{Rxn1}	heat of reaction per mol of H_2 consumed going to left for reaction 1
ΔH_{Rxn2}	heat of reaction per mole of H_2 consumed going to left for reaction 2
ε	void fraction (porosity) of particle bed
μ	viscosity of H_2, Pa s
ρ	mass density, kg/m^3
ρ_{bed}	bulk mass density of bed; kg/m^3 $= (1-\varepsilon)\rho_{bed-particule}$ =mass of solid/total volume
$\rho_{bed-particule}$	particle mass density of bed, kg/m^3=mass of solid/volume of solid
$\rho_{bed} C_{p\ bed}$	$\rho_{\text{Solid Reactants}} C_{p\text{Solid Reactants}} + \rho_{\text{Solid Products}} C_{p\text{Solid Products}}$
ρ_{H_2}	hydrogen density, kg/m^3
ρ_{metal}	density of the metal, kg/m^3

Symbol and operators

∇	gradient, 1/m.

REFERENCES

[1] Satyapal, S., Read, C., Thomas, G., and Ordaz, G., 2007, "The U.S. Department of Energy's National Hydrogen Storage Project: Progress Towards Meeting Hydrogen-Powered Vehicle Requirements", Catalysis Today, **120**(3-4), pp. 246-256.

[2] Demircan, A., Kaplan, Y., Mat, M. D., and Veziroglu, T. N., 2005, "Experimental and Theoretical Analysis of Hydrogen

Absorption in $LaNi_5$-H_2 Reactors", International Journal of Hydrogen Energy, **30**(13-14), pp. 1437-1446.
[3] Ataer, Ö. E., and Bilgili, M., 2005, "Numerical Analysis of Hydrogen Absorption in a P/M Metal Bed", Powder Technology. **160**(2), pp. 141-148.
[4] Dogan, A., Kaplan, Y., and Veziroglu, T. N., 2004, "Numerical Investigation of Heat and Mass Transfer in a Metal Hydride Bed", Applied Mathematics and Computation, **150**(1), pp. 169-180.
[5] Kikkinides, E. S., Georgiadis, M. C., and Stubos, A. K., 2006, "Dynamic Modelling and Optimization of Hydrogen Storage in Metal Hydride Beds", Energy, **31**(13): p. 2428-2446.
[6] Kikkinides, E. S., Georgiadis, M. C., and Stubos, A. K., 2006, "On the Optimization of Hydrogen Storage in Metal Hydride Bed", International Journal of Hydrogen Energy, **31**(6), pp. 737-751.
[7] MacDonald, B. D., Rowe, A. M., 2006, "A Thermally Coupled Metal Hydride Hydrogen Storage and Fuel Cell System", Journal of Power Sources,**161**, pp. 346-355.
[8] Askri, F., Ben Salah, M., Jemni, A., and Ben Nasrallah, S., 2009, "Optimization of Hydrogen Storage in Metal-Hydride Tanks", International Journal of Hydrogen Energy, **34**(2), pp. 897-905.
[9] Mellouli, S., Dhaou, H., Askri, F., Jemni, A., and Ben Nasrallah, S., 2009, "Hydrogen Storage in Metal Hydride Tanks Equipped with Metal Foam Heat Exchanger", International Journal of Hydrogen Energy, **34**(23), pp. 9393-9401.
[10] Chaise, A., De Rango, P., Marty, Ph., Fruchart, D., Miraglia, S., Olivès, R., and Garrier, S., 2009, "Enhancement of Hydrogen Sorption in Magnesium Hydride Using Expanded Natural Graphite", International Journal of Hydrogen Energy, **34**(20), pp. 8589-8596.
[11] Mellouli, S., Askri, F., Dhaou, H., Jemni, A., and Ben Nasrallah, S., 2007, "A Novel Design of a Heat Exchanger for a Metal-Hydrogen Reactor", International Journal of Hydrogen Energy, **32**(15): p. 3501-3507.
[12] Mellouli, S., Askri, F., Dhaou, H., Jemni, A., and Ben Nasrallah, S., 2009, "Numerical Study of Heat Exchanger Effects on Charge/Discharge Times of Metal-Hydrogen Storage Vessel", International Journal of Hydrogen Energy, **34**(7), pp. 3005-3017.
[13] Mohan, G., Maiya, M. P., and Murthy, S. S., 2007, "Performance Simulation of Metal Hydride Hydrogen Storage Device with Embedded Filters and Heat Exchanger Tubes", International Journal of Hydrogen Energy, **32**,pp. 4978 - 4987.
[14] Krokos, C. A., Nikolic, D., Kikkinides, E. S., Georgiadis, M. C, and Stubos, A. K., 2009, "Modeling and Optimization of Multi-tubular Metal Hydride Beds for Efficient Hydrogen Storage", International Journal of Hydrogen Energy, **In Press**.
[15] Hardy, B. J., and Anton, D. L., 2009, "Hierarchical Methodology for Modeling Hydrogen Storage Systems. Part I: Scoping Models", International Journal of Hydrogen Energy, **34**(5), pp. 2269-2277.
[16] Hardy, B. J., and Anton, D. L., 2009, "Hierarchical Methodology for Modeling Hydrogen Storage Systems. Part II: Detailed Models", International Journal of Hydrogen Energy, **34**(7), pp. 2992-3004.
[17] Mosher, D.A., Arsenault, S., Tang, X., and Anton, D.L., 2007, "Design, Fabrication and Testing of $NaAlH_4$ Based Hydrogen Storage Systems", Journal of Alloys and Compounds, **446-447**, pp. 707-712.
[18] COMSOL Multiphysics, v.a.C.-C.A. version 3.5a. Copyright 1998-2008. COMSOL AB.